ISSN 1674-1056
http://cpb.iphy.ac.cn
http://iopscience.iop.org/cpb
中国物理 B
Chinese Physics
中国物理 Chinese Physics B

Current loss of magnetically insulated coaxial diode with cathode negative ion

Dan-Ni Zhu(朱丹妮), Jun Zhang(张军), Hui-Huang Zhong(钟辉煌), Jing-Ming Gao(高景明), Zhen Bai(白珍)
Citation: Chin. Phys. B . 2018, 27(2): 020501. **doi:** 10.1088/1674-1056/27/2/020501

Journal homepage: http://cpb.iphy.ac.cn; http://iopscience.iop.org/cpb

What follows is a list of articles you may be interested in

Pattern dynamics of network-organized system with cross-diffusion

Qianqian Zheng(郑前前), Zhijie Wang(王直杰), Jianwei Shen(申建伟)
Chin. Phys. B . 2017, 26(2): 020501. **doi:** 10.1088/1674-1056/26/2/020501

Analysis of field coupling to transmission lines with random rotation over the ground

Xie Hai-Yan, Li Yong, Qiao Hai-Liang, Wang Jian-Guo
Chin. Phys. B . 2015, 24(6): 060501. **doi:** 10.1088/1674-1056/24/6/060501

A generalized Padé approximation method of solving homoclinic and heteroclinic orbits of strongly nonlinear autonomous oscillators

Li Zhen-Bo, Tang Jia-Shi, Cai Ping
Chin. Phys. B . 2014, 23(12): 120501. **doi:** 10.1088/1674-1056/23/12/120501

Current loss of magnetically insulated coaxial diode with cathode negative ion

Dan-Ni Zhu(朱丹妮)†, Jun Zhang(张军)‡, Hui-Huang Zhong(钟辉煌), Jing-Ming Gao(高景明), and Zhen Bai(白珍)

College of Optoelectronic Science and Engineering, National University of Defense Technology, Changsha 410073, *China*

(Received 3 August 2017; revised manuscript received 16 October 2017; published online 5 January 2018)

Current loss without an obvious impedance collapse in the magnetically insulated coaxial diode (MICD) is studied through experiment and particle-in-cell (PIC) simulation when the guiding magnetic field is strong enough. Cathode negative ions are clarified to be the predominant reason for it. Theoretical analysis and simulation both indicate that the velocity of the negative ion reaches up to 1 cm/ns due to the space potential between the anode and cathode gap (A–C gap). Accordingly, instead of the reverse current loss and the parasitic current loss, the negative ion loss appears during the whole pulse. The negative ion current loss is determined by its ionization production rate. It increases with diode voltage increasing. The smaller space charge effect caused by the beam thickening and the weaker radial restriction both promote the negative ion production under a lower magnetic field. Therefore, as the magnetic field increases, the current loss gradually decreases until the beam thickening nearly stops.

Keywords: magnetically insulated coaxial diode (MICD), cathode plasma, negative ion, current loss

PACS: 05.10.–a, 07.05.–t, 07.30.–t, 11.40.–q **DOI:** 10.1088/1674-1056/27/2/020501

1. Introduction

Magnetically insulated coaxial diode (MICD) is advantageous to generate an intense annular beam with extensive applications in high power microwave (HPM) systems, especially for the O-type HPM generator.[1–5] MICD provides an electron beam from the boundary of the plasma formed at the surface of the cathode.[6] Its current transmission characteristics directly influence the power conversion efficiency of the HPM source. Apart from the divergence loss of the electron beam, the radial expansion of cathode plasma is assumed to cause the current loss under a low magnetic field.[7,8] Reverse electron current is unavoidable for MICD in the transition region before the uniform axial magnetic field, that is, a portion of electrons which stem from the stray emission on the cathode move in cycloidal orbits following a magnetic force line in a direction opposite to the downstream primary electron flow.[9,10] Some researchers found that the reverse electron current could cross the diode anode and cathode gap (A–C gap) and be absorbed by the anode in the diode transition region, resulting in the reverse current loss.[7,11,12]

The others considered that the extra electron emission occurred on the external ring of a shield hoop, which leads to a parasitic current loss especially when the reverse current flows on the shield hoop.[13] The above current losses all appearance with the diode impedance collapsing. However, an insulated MICD still has an over 10% current loss in a strong guiding magnetic field without apparent diode impedance collapsing in the experiment. There has been no physical explanation to it.

In this paper, we try to give a reasonable explanation to the current loss involving the cathode negative ion. An experimental platform of MICD electrical diagnostics with four Rogowski coils at different positions along the MICD is designed. The axial guiding magnetic field including its profile lines and strength and the shield hoop are well shaped to avoid the mentioned current loss in our experiment. The attention is paid to the current loss relating to the cathode negative ion. The rest of this paper is organized as follows. In Section 2, we discuss the details of the experimental setup and diagnostics. A corresponding particle-in-cell (PIC) simulation MICD model including the cathode plasma and the negative ion is built in Section 3 to confirm the phenomenon of cathode negative ion loss. The negative ion velocity is estimated in both theory and simulation. The comparison between the experimental results and simulation results develops a physical understanding of the current loss when the magnetic field increases. Finally, some conclusions are drawn from the present study in Section 4.

2. Experimental setup and diagnostics

Based on an intensive current e-beam accelerator, the experiment about current loss was performed as shown in Fig. 1.[14] The electron beam was emitted from an annular graphite cathode, accelerated towards the anode tube, and then collected by the collector. Solenoid magnet coils provided an axial guiding magnetic field. The magnetic field strength (B)

†Corresponding author. E-mail: 360681625@qq.com
‡Corresponding author. E-mail: junzhang@nudt.edu.cn

© 2018 Chinese Physical Society and IOP Publishing Ltd

in the uniform region increased from 0.2 T to 1.8 T by adjusting the solenoid current. The shunting reverse current in the MICD was emitted by the cylindrical side surface of the graphite cathode.[10] A shield hoop was introduced to protect the insulator from being bombarded by the reverse electron beam[13,15,16] as shown in Fig. 1. Consequently, there was no such reverse current loss as described in Refs. [7], [11], and [12]. The outer radius of the annular graphite cathode R_c was 2.8 cm with a blade width of 0.15 cm. The radius of the magnetic solenoid hole R_a, the radius of the cutoff neckR_p, and the radius of the anode drift tube were 6 cm, 3.4 cm, and 3.3 cm, respectively.

The diode voltage was monitored by a capacitive–voltage divider between the insulator and the shield hoop. The current signals at different positions along the MICD were measured by four Rogowski coils, which were calibrated before the experiment. Rogowski coil 1, Rogowski coil 2, Rogowski coil 3, and Rogowski coil 4 were installed in front of the shield hoop, on the left side of the guiding magnetic solenoid, between the cutoff neck and the anode drift tube, at the entrance of the collector, respectively. The reverse electron beam passing along the magnetic force line ends at the shield hoop to the right side of Rogowski coil 1. The Rogowski coil 1 could record the total diode current I_0.[7] Rogowski coil 2 and Rogowski coil 3 monitored the diode currents just in front of the guiding magnetic solenoid (I_g) and the forward beam current through the drift tube involving beam-wave interaction (I_n), respectively. The collected forward beam current I_c that arrived at the entrance of the collector was measured by Rogowski coil 4. The waveforms of the diode voltage (U) and the currents (I_0, I_g, I_n, and I_c) at 1.0 T are shown in Fig. 2, which represents the typical case that the diode has achieved magnetic insulation.

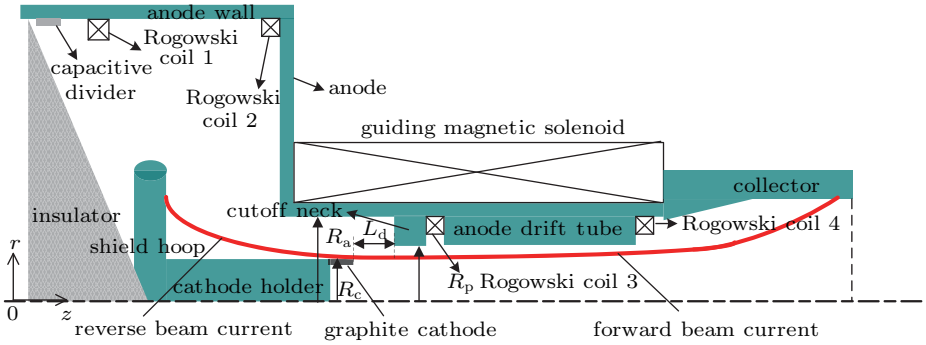


Fig. 1. (color online) Schematic diagram of the experiment setup of MICD. The red lines denote the annular electron beam. (R_c = 2.8 cm, R_a = 6 cm, and R_p = 3.4 cm).

On the one hand, I_g has almost the same waveform and amplitude as I_0 in Fig. 2, denoting no parasitic current loss. On the other hand, I_n nearly equals I_c, demonstrating that the electron beam transmission efficiency through the anode drift tube is close to 100%. Then the diode current I_t, the forward beam current I_b, and the current loss coefficient K are defined as $I_t = (I_0 + I_g)/2$, $I_b = (I_n + I_c)/2$, and $K = 1 - I_b/I_t$, respectively.

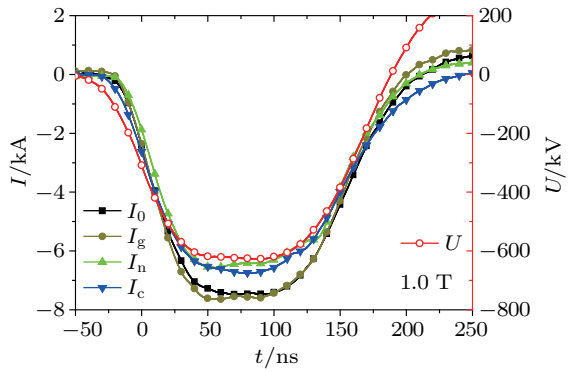


Fig. 2. (color online) Waveforms of current at different positions and diode voltage at B = 1.0 T.

Figure 3 displays the variations of the diode current, the forward beam current, and the current loss coefficient with guiding magnetic field strength in the experiment. It validates that the electron beam is confined, when the guiding magnetic field strength B is not below the critical value (B = 0.4 T) for which the magnetic insulation is realized.[17,18] However, the current loss coefficient maintains 10%∼20% (Fig. 3) and the waveforms of the current at different positions and the diode voltage are almost stable during the main part of the pulse as shown in Fig. 2 when $B \geq 0.4$ T. It should be noticed that the current loss appears during the whole pulse. Moreover, the current loss cannot be totally eliminated by the strong magnetic field.

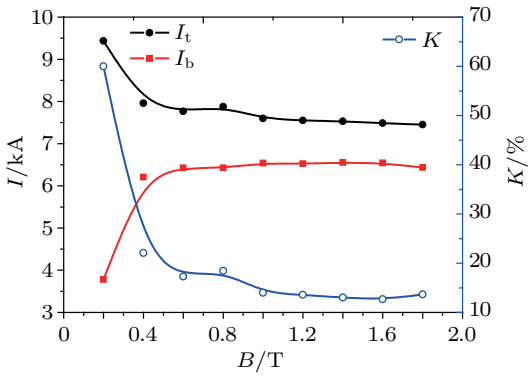


Fig. 3. (color online) Plots of diode current, forward beam current and current loss coefficient versus guiding magnetic field strength in experiment.

3. Discussion about current loss with MICD PIC simulation

The characteristics of current loss described in Section 2 suggest that the loss is also possibly caused by the negative ion from the cathode in this MICD.[19] In fact, the explosive emission of the cathode surface is very complex. Besides electrons and positive ions, there are also negative ions in plasma on the cathode surface. The negative ions including H^-, C^-, O^-, etc.[19–21] are regarded as the main cause for the current loss.[20–23] In a vacuum, the source of negative ions is the absorbed gas whose main components are hydrogen and hydrocarbon[19–21,24] in the cathode. The desorption of gas molecules gains energy from Ohmic heating, electric potential, and the return ion bombardment.[25] These desorbed gas molecules become negative ions in two ways.[20] Firstly, when electrons impact the molecules, negative ions may be produced[26–28] with some probabilities. Secondly, because of the explosive emission of the cathode surface, a lot of plasma are produced and would bombard the cathode surface. The dominant negative ion production mechanism from these desorbed gas molecules is backscattering of the cathode plasma ions incident on the cathode surface at energies greater than a few eV.[22] It is relatively easy for the heavy negative ions to be produced and cross the A–C gap due to the effect of the electric field even in a strong magnetic field. The velocity is so high of about 1 cm/ns[22] that once negative ions are produced, they can arrive at the anode, leading to a subsequent current loss quickly.

3.1. PIC simulation models

Firstly, a 2.5-D PIC simulation model ignoring the cathode plasma and cathode negative ion is constructed according to the structure and parameters of the MICD in experiment. A voltage pulse of about 625 kV is exerted on the anode–cathode gap to generate the electrons. The current signals at different positions along the MICD in experiment are recorded in the simulation. Figure 4 shows the variations of average amplitudes of diode current, forward beam current and current loss coefficient with magnetic field strength in the simulation. Only when $B < 0.4$ T, will an obvious current loss occur as the electron beam disperses and the diode gap closure happens. When $B \geq 0.4$ T, the diode current equals the forward beam current in Fig. 4. This amplitude is nearly coherent with that of the forward beam current in the experiment (Fig. 3).

Then the cathode plasma and cathode negative ion are considered in the PIC simulation model. Because water vapor is most common in the desorbed gas, only H^+ and H^- are assumed to be existent in the following simulations for simplification. A hydrogen gas layer with a thickness of two mesh sizes covers on the cylindrical side and end surface of the cathode. In this model, the movements of neutral particles and their mutual interactions are neglected for simplicity.[29,30] Based on the electron impact-ionization model,[29–31] the cathode plasma including ions and electrons are generated when an electron beam propagates through the neutral gas layer and ionizes the gas. Similarly, the cathode negative ions (H^-) are produced when the backscattering ions (H^+) bombard and ionize the residual neutral gas according to the ion impact-ionization model as the dominant negative ion production mechanism.[22]

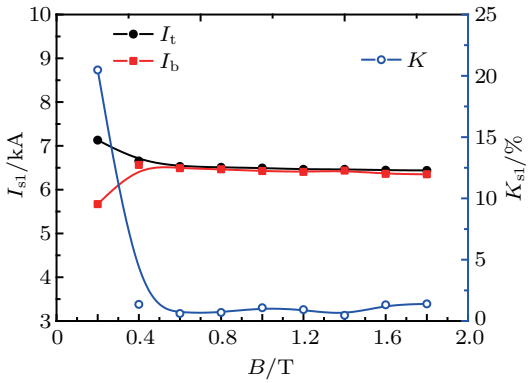


Fig. 4. (color online) Plots of average variations of diode current, forward beam current and current loss coefficient versus guiding magnetic field strength in simulation without cathode plasma or negative ion.

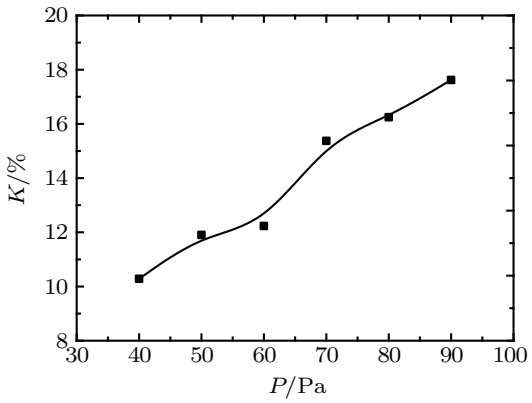


Fig. 5. Plots of current loss coefficient versus neutral gas pressure in the impact-ionization model at 1.8 T.

Obviously, the negative ion current depends on its ionization production rate. From the experimental results, the relationship between loss current density and input current density follows approximately a power law.[20] As a result, the negative ion current loss is determined by its ionization production rate. The ionization production rate is defined as[30]

$$R_{\text{ion}} = n_{\text{t}} \phi_{\text{i}} \sigma_{\text{ion}}, \tag{1}$$

where ϕ_{i} denotes the incident particle flux, which relates to the incident current density. σ_{ion} is the total cross section for impact ionization involving the target neutral species, and n_{t} is the target neutral number density and expressed as

$$n_{\text{t}} = P/kT, \tag{2}$$

with k, P, and T representing the Boltzmann constant, the target neutral gas pressure, and temperature, respectively. The gas temperature T in the impact-ionization model is usually 300 K.[30] It is difficult to estimate the gas pressure and is limited by the PIC simulation calculation capability. Figure 5 shows the variations of the current loss coefficient K with gas pressure in the impact-ionization model. The ionization production rate is proportional to gas pressure according to Eqs. (1) and (2). Therefore, that the larger P promotes more serious negative ion loss in the ion impact-ionization model can be explained. Similarly, the larger the P, the more plasma ions are generated in the electron impact-ionization model, thereby leading to the larger incident ion current density in the ion impact-ionization model. Therefore, K increases with P increasing based on Eq. (1). The value of P is set to be 60 Pa in the model for which the diode voltage, the current, and K are close to the experimental results. In fact, the negative ion density is source limited rather than space charge limited.[22] Thus the negative ion current loss is a function sensitive to the factors which affect the cathode plasma, such as electric field, sheath current, and surface preparation[19,22] through the incident particle flux.

3.2. Calculation of negative ion velocity

The contour lines of the electric field distribution across the A–C gap region of the MICD are illustrated in Fig. 6. Figures 7 and 8 display the space distributions of all the charged particles, the negative ions, and the positive ions in the MICD model with 1.0 T at different moments. The cathode negative ions are not confined by the magnetic field but transmit towards the anode tube along the electric field lines across the A–C gap as indicated in Fig. 6. Figures 7(b) and 8(b) demonstrate that it takes 3.3 ns for the negative ion to move a trajectory of about 3.4 cm from the cathode to the anode tube. Therefore, the average velocity is about 1.1 cm/ns. As the positive ion expansion velocity is just several cm/μs,[29,30] its expansion is not obvious during the period as shown in Figs. 7(c) and 8(c).

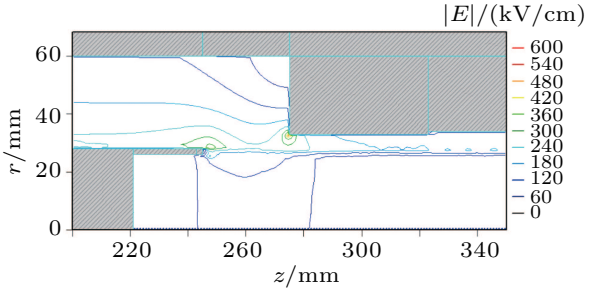


Fig. 6. (color online) Contour lines of the electric field distribution across the A–C gap region of the MICD.

The average negative ion velocity that depends on the space potential across the A–C gap can be calculated by ignoring the weak influence of the magnetic field as follows:[31]

$$\upsilon_{\mathrm{n}} = \sqrt{2\,|\varphi(R_{\mathrm{c}})q|/m_{\mathrm{n}}}, \tag{3}$$

where m_{n} and q are the mass and the charge of the negative ion. The space potential difference across the A–C gap in Fig. 5 is estimated from[32]

$$\varphi(R_{\mathrm{c}}) = \frac{I_{\mathrm{b}}}{2\pi\varepsilon_0\upsilon_{\mathrm{b}}}\ln(R_{\mathrm{c}}/R_{\mathrm{a}}), \tag{4}$$

where ε_0 is the permittivity of a vacuum, υ_{b} is the axial velocity of the electron, R_{c} equals the beam outer radius, and R_{a} is the magnetic solenoid hole radius. The forward beam current is defined as[32]

$$I_{\mathrm{b}} = \frac{17.1\ kA}{2\ln(R_{\mathrm{a}}/R_{\mathrm{c}})}\left(\gamma_{\mathrm{b}}^2-1\right)^{1/2}\frac{\gamma-\gamma_{\mathrm{b}}}{\gamma_{\mathrm{b}}}, \tag{5}$$

including

$$\gamma_{\mathrm{b}} = \left(1-\upsilon_{\mathrm{b}}^2/c^2\right)^{-1/2}, \tag{6}$$

$$\gamma = 1+|eU|/mc^2, \tag{7}$$

where U denotes the diode voltage, e and m are the mass and the charge of electron, respectively, and c is the speed of light. For the case of H^- at 1.0 T, $U = 625$ kV, $I_{\mathrm{b}} = 6.6$ kA, $q = e = 1.6\times10^{-19}$ C, $m_{\mathrm{n}} = 1.67\times10^{-27}$ kg, $m = 9.11\times10^{-31}$ kg, $R_{\mathrm{c}} = 2.8$ cm, and $R_{\mathrm{a}} = 6$ cm. When these parameters are substituted, $\upsilon_{\mathrm{b}} = 11.1$ cm/ns. Then the average negative ion velocity υ_{n} is about 1.25 cm/ns. It is a little larger than the value estimated from Figs. 6 and 7, which is attributed to the ignorance of the suppression effect from the magnetic field.

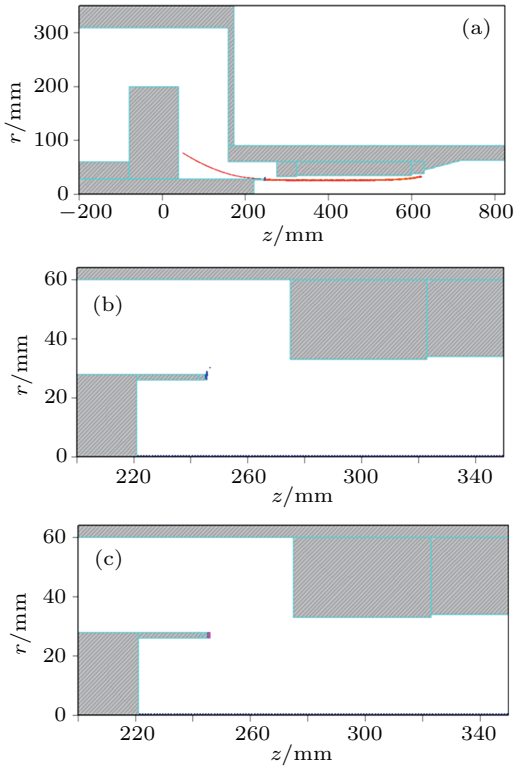


Fig. 7. (color online) Distributions in the PIC simulation diode with 1.0 T at 4.5 ns of (a) all charged particles, (b) negative ions, and (c) positive ions.

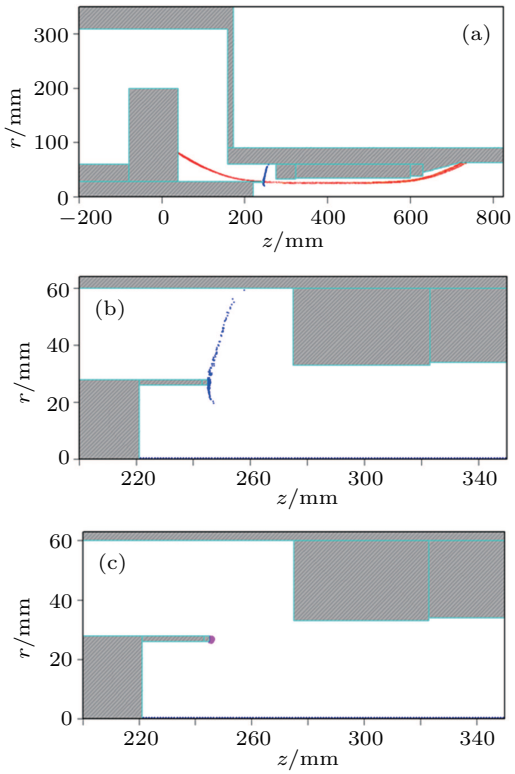


Fig. 8. (color online) Distribution in the PIC simulation diode with 1.0 T at 7.8 ns of (a) all charged particles, (b) negative ions, and (c) positive ions.

3.3. Influence of magnetic field

The variations of the diode current, forward beam current, and current loss coefficient with guiding magnetic field strength involving the cathode plasma and the negative ion are illustrated in Fig. 9. This simulation result includes the fact that the current loss coefficient maintains about 12% when $B \geq 1.0$ T, which well agrees with the experiment result in Fig. 3. It proves that the current loss is mainly attributed to the negative ion when the guiding magnetic field is strong enough.

In all, the strong magnetic field is unable to totally confine the negative ions because of the relatively large ion mass. Furthermore, the negative ion is able to rapidly cross the A–C gap due to the electric field and be absorbed by the anode, resulting in a current loss as shown in Figs. 3 and 9.

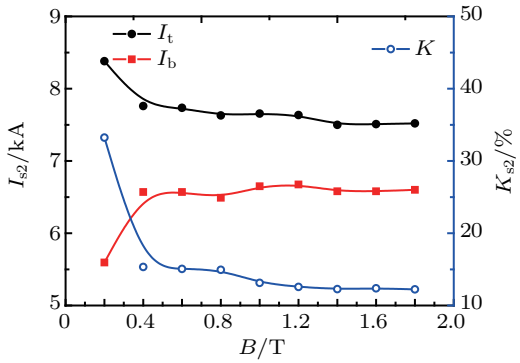


Fig. 9. (color online) Variations of diode current, forward beam current, and current loss coefficient with guiding magnetic field strength in simulation with considering cathode plasma and negative ions.

Variations in the experiment refer to the fact that the current loss coefficient decreases slightly with the growing magnetic field until $B = 1.0$ T, which is confirmed in Fig. 9. An extremely low guiding magnetic field leads to beam thickening caused by the large cyclotron radius of the electron.[33,34] Then the leading role in the beam thickening is played by the radial plasma expansion due to the relatively small cyclotron radius of the electron by further increasing the magnetic field.[33,34] The beam thickening would weaken the space charge effect.[8] Hence the small space charge effect and the weak radial restriction in the lower magnetic field both promote more plasma ions to return and ionize the neutral gas, resulting in a larger negative ion production rate. Consequently, the current loss coefficient increases with magnetic field decreasing. As the radial plasma expansion nearly almost stops when the magnetic field is over 1.0 T, the beam thickness is still a small value due to a large radial restriction.

The current loss in experiment (Fig. 3) is a bit larger than that of the simulation especially for $B \leq 1.0$ T (Fig. 9), which is suspected to be caused by the anode plasma. When negative ions with a significant current density bombard the anode, they may create the anode tube plasma and contribute to the rapid impedance collapse in beam diode as the power density and the rate-of-voltage change are increased.[19,20] However, we do not observe an apparent impedance collapse except in the case of 0.2 T. The cathode negative ions and the anode plasma may be the main factors leading to the current loss.[20] The effect of the anode plasma from the anode tube wall except for that formed at the collector[31] will be studied further.

3.4. Influence of diode voltage

Figure 10 displays the current loss coefficients under different diode voltages at 1.0 T in the experiment and the above two impact-ionization simulation models. The higher the diode voltage, the larger the incident particle flux and the ionization production rate based on Eq. (1). As a result, the negative ion current loss coefficient increases with diode voltage increasing as illustrated in both experiment and simulation.

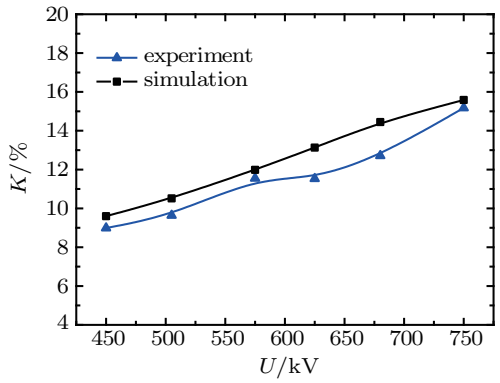


Fig. 10. (color online) Plots of current loss coefficient versus diode voltage in experiment and simulation at 1.0 T.

4. Conclusions

The current loss of MICD, when the magnetic field is enhanced, is investigated through experiment, PIC simulation, and physical analysis, demonstrating general agreements among them. Apart from the reverse current loss and the parasitic current loss, the significant current loss in a strong magnetic field is mainly attributed to the cathode negative ions. The negative ion loss tends to exist during the whole pulse due to its high velocity (reaching up to l cm/ns). Even when the electrons in the MICD are magnetically insulated, the negative ions dump on the anode because of their relatively large ion mass and the electric field across the A–C gap. The negative ion current loss is determined by its ionization production rate. It increases with the rise of diode voltage. Besides, the current loss gradually decreases when the magnetic field increases until the beam thickening stops, because the smaller space charge effect caused by the beam thickening and the weaker radial restriction both contribute to the high negative ion production rate under low magnetic field.

References

[1] Zhang J, Zhong H and Luo L 2004 *IEEE Trans. Plasma Sci.* **32** 236
[2] Qi Z, Zhang J, Zhang Q, Zhong H, Xu L and Yang L 2016 *IEEE Electron Dev. Lett.* **37** 782
[3] Bai Z, Zhang J and Zhong H 2016 *Phys. Plasmas* **23** 043109
[4] Zhang D, Zhang J, Zhong H and Jin Z 2012 *Phys. Plasmas* **19** 103102
[5] Zhu D, Zhang J, Zhong H, Jin Z and Qi Z 2015 *Phys. Plasmas* **22** 113301
[6] Miller R B 1982 *An Introduction to the Physics of Intense Charged Particle Beams* (New York: Plenum Press)
[7] Xiao R, Sun J, Huo S, Li X, Zhang L, Zhang X and Zhang L 2010 *Phys. Plasmas* **17** 123107
[8] Wu P, Sun J and Ye H 2015 *Phys. Plasmas* **22** 63109
[9] Miller R B, Prestwich K R, Poukey J W and Shope S L 1980 *J. Appl. Phys.* **51** 3506
[10] Yalandin M I, Mesyats G A, Rostov V V, Sharypov K A, Shpak V G, Shunailov S A and Ulmaskulov M R 2015 *Appl. Phys. Lett.* **106** 233504
[11] Sun J, Zhang Y, Song Z, Zhang X and Chen C 2013 *Mod. Appl. Phys.* **4** 246 (in Chinese)
[12] Sheffield R L, Montgomery M D, Parker J V and Riepe K B 1982 *J. Appl. Phys.* **53** 5408
[13] Xiang F, Li C and Tan J 2011 *High Power Laser and Particle Beams.* **23** 831 (in Chinese)
[14] Ge X, Zhong H, Qian B, Zhang J, Liu L, Gao L, Yuan C and He J 2010 *Appl. Phys. Lett.* **97** 241501
[15] Liu X 2005 *High pulsed power technology* (Beijing: National Defense Industry) (in Chinese)
[16] Zhang Y H, Ma Q S, Chang A, Zhou C M, Gan Y Q and Liu Z 2004 *High Power Laser and Particle Beams* **16** 1437 (in Chinese)
[17] Jones M E, Mostrom M A and Thode L E 1981 *J. Appl. Phys.* **52** 4942
[18] Lovelace R V and Ott E 1974 *Phys. Fluids* **17** 1263
[19] Van Devender J P, Stinnett R W and Anderson R J 1981 *Appl. Phys. Lett.* **38** 229
[20] Wu H, Zeng Z, Wang L and Guo N 2014 *Plasma Sci. Technol.* **16** 625
[21] Baker D H, Doverspike L D and Champion R L 1992 *Phys. Rev. A* **46** 296
[22] Regan W Stinnett and Tim Stanley 1982 *J. Appl. Phys.* **53** 3819
[23] Wu H, Zeng Z, Guo N, Zhang X, Lei T, Han J, Hu Y, Sun T and Wang L 2012 *IEEE Trans. Plasma Sci.* **40** 1177
[24] Marton and LadislausLaszlo 1979 *Methods of experimental physics*: *Vacuum physics and technology*, Vol. 14 (Academic Press)
[25] Schwirzke F, Hallal M P and Maruyama X K 1993 *IEEE Trans. Plasma Sci.* **21** 410
[26] Gerber A and Herzenberg A 1985 *Phys. Rev. B* **31** 6219
[27] Rous P J 1995 *Phys. Rev. Lett.* **74** 1835
[28] Ottinger P F and Schumer J W 2006 *Phys. Plasmas* **13** 63109
[29] Zhu D, Zhang J, Zhong H and Cai D 2016 *Phys. Plasmas* **23** 81503
[30] Xu Q, Liu L 2012 *Phys. Plasmas* **19** 093111
[31] Xiao R, Chen C, Deng Y, Cao Y, Sun J and Li J 2016 *Phys. Plasmas* **23** 63114
[32] Swegle J A, Poukey J W and Leifeste G T 1985 *Phys. Fluids* **28** 2882
[33] Belomyttsev S Y, Rostov V V, Romanchenko I V, Shunailov S A, Kolomiets M D, Mesyats G A, Sharypov K A, Shpak V G, Ulmaskulov M R and Yalandin M I 2016 *J. Appl. Phys.* **119** 23304
[34] Korovin S D and Pegel I V 2012 *International Conference on High-Power Particle Beams*, 30 September–5 October, 2012, Karlsruhe, Germany